JOURNAL OF APPLIED ELECTROCHEMISTRY 20 (1990) 32–38

Transition metal-based hydrogen electrodes in alkaline solution — electrocatalysis on nickel based binary alloy coatings

I. ARUL RAJ, K. I. VASU

Central Electrochemical Research Institute, Karaikudi 623 006, India

Received 23 November 1988; revised 14 April 1989

Nickel–molybdenum, nickel–zinc, nickel–cobalt, nickel–tungsten, nickel–iron and nickel chromium binary alloy codeposits, obtained through electrodeposition methods on mild steel strips, have been characterized with the objective of qualitatively comparing and assessing their electrocatalytic activities as hydrogen electrodes in alkaline solution. It has been concluded that their electrocatalytic effects for the hydrogen evolution reaction rank in the following order: Ni–Mo > Ni–Zn (after leaching Zn in KOH) > Ni–Co > Ni–W > Ni–Fe > Ni–Cr > Ni plated steel. Further investigations on the alloy electrocatalysts have revealed that the cathodic overpotential contribution to the electrolysis voltage can be brought down by 0.3 V when compared with conventional cathodes. The best and most stable hydrogen evolving cathode, based on nickel–molybdenum alloy, exhibited an overpotential of about 0.18 V for over 1500 h of continuous electrolysis in 6 M KOH at 300 mA cm^{-2} and 353 K. The salient features of the coatings, such as physical characteristics, chemical composition, crystal structure of the alloy phases and the varying effects of the catalytic activation method were analysed with a view to correlating the micro-structural characteristics of the coatings with the hydrogen adsorption process. The stability under open-circuit conditions, the tolerance to electrochemical corrosion and the long term stability of nickel–molybdenum alloy cathodes were very encouraging. An attempt to identify the pathway for the hydrogen evolution reaction on these alloy coatings was made, in view of the very low apparent activation energy values obtained experimentally.

1. Introduction

In continuing our search for electrocatalytic materials for hydrogen and oxygen electrodes based on transition metals in alkaline solution [1–3], along with various other groups [4–9], we report here the results of our experiments on some binary alloy codeposits based on nickel–molybdenum/zinc/cobalt/tungsten/iron/chromium, as hydrogen evolving cathodes in alkaline solution. A discussion on the physical characteristics of the coatings, reverse potential cycling effects, results of life tests by simulation experiments and the electrochemical parameters for the hydrogen evolution reaction on these coatings has been included.

2. Experimental details

2.1. *Pretreatment and deposition processes*

Mild steel foils of composition C = 0.06 %, Si = 0.04 %, Mn = 0.3 %, P = 0.002 %, Cr = 0.003 %, Ni = 0.008 % and Mo = 0.006 % were cut into 20 cm × 5 cm rectangular strips. The shearing edges of the strips were machined to a smooth finish. The pretreatment procedure involved initial mechanical surface polishing to a mirror finish using fine emery cloth (John Oakey) followed by sand blasting. Then the surfaces were washed, dried and thoroughly degreased with acetone followed by washing in triple distilled water. This was followed by cathodic cleaning in an alkaline bath containing sodium hydroxide 40 %, sodium silicate 10 % and sodium phosphate 10 % at 353 K and 100 mA cm^{-2} current density for 3 min. This was followed by anodic and again cathodic cleaning under similar conditions. Before electrodeposition, each substrate was washed thoroughly using triple distilled water.

The deposition processes were carried out using geometric area of 130 cm^2 (two sides), masking the rest with alkali resistant epoxy resin under galvanostatic steady state conditions, using two thin rectangular graphite strips as anodes, on both sides of the cathodes. The anodes were contained in Nylon bags. The details of the bath and the deposition conditions are presented in Table 1. Each alloy deposition was carried out on three similar substrates under idential conditions.

2.2. *SEM, XRD and AAS experiments*

The surface microstructures of the alloy coatings were investigated using scanning electron microscopy (SEM, JEOL JSM 35 CF). The chemical composition of each alloy coating was obtained by using the

0021-891X/90 $03.00 + .12

Table 1. Bath characteristics and operating conditions for electrolytic codeposition

Ni–Mo		*Ni–W*		*Ni–Zn*	
Parameters	*Values*	*Parameters*	*Values*	*Parameters*	*Values*
$NiSO_4 . 6H_2O$	80 g pl	$NiSO_4 . 6H_2O$	80 g pl	$NiSO_4 . 6H_2O$	150 g pl
$Na_2MoO_4 . 2H_2O$	20 g pl	$Na_2WO_4 . 2H_2O$	20 g pl	$ZnSO_4 . 7H_2O$	40 g pl
$K_3C_6H_5O_7 . H_2O$	50 g pl	$K_3C_6H_5O_7 . H_2O$	50 g pl	NH_4Cl	30 g pl
Na_2CO_3	Excess	Na_2CO_3	Excess	CH_3COONa	30 g pl
pH	10.5	pH	10.5	H_3BO_3	15 g pl
				pH	5.5 to 6.5
Temperature	301 K	Temperature	301 K	Temperature	333 K
Current density	10 mA cm^{-2}	Current density	10 mA cm^{-2}	Current density	5 mA cm^{-2}
Duration	90 min	Duration	90 min	Duration	90 min
Agitation	250 r p m	Agitation	250 r p m	Agitation	250 r p m
Cathode efficiency	25%	Cathode efficiency	15%	Cathode efficiency	25%
Weight of deposit	3.6 mg cm^{-2}	Weight of deposit	3.0 mg cm^{-2}	Weight of deposit	4.0 mg cm^{-2}
Thickness of deposit	2.5–4.0 μm	Thickness of deposit	3.6 μm	Thickness of deposit	5–7.0 μm
Colour of deposit	Grey	Colour of deposit	Pale black	Colour of deposit	Dull white
Adhesion	Very good	Adhesion	Very good	Adhesion	Very good

Ni–Fe		*Ni–Co*		*Ni–Cr*	
Parameters	*Values*	*Parameters*	*Values*	*Parameters*	*Values*
$NiSO_4 . 6H_2O$	80 g pl	$NiSO_4 . 6H_2O$	80 g pl	$NiSO_4 . 6H_2O$	80 g pl
$FeSO_4 . 7H_2O$	20 g pl	$CoSO_4 . 7H_20$	20 g pl	CrO_3(Dil HNO_3)	20 g pl
$K_3C_6H_5O_7 . H_2O$	50 g pl	$K_3C_6H_5O_7 . H_2O$	50 g pl	$K_3C_6H_5O_7 . H_2O$	50 g pl
Na_2CO_3	Excess	Na_2CO_3	Excess	Na_2CO_3	Excess
pH	10.5	pH 10.5	10.5	pH	10.5
Temperature	301 K	Temperature	301 K	Temperature	301 K
Current density	10 mA cm^{-2}	Current density	10 mA cm^{-2}	Current density	10 mA cm^{-2}
Duration	90 min	Duration	90 min	Duration	90 min
Agitation	250 r p m	Agitation	250 r p m	Agitation	250 r p m
Cathode efficiency	25%	Cathode efficiency	50%	Cathode efficiency	25%
Weight of deposit	5.1 mg cm^{-2}	Weight of deposit	10–11 mg cm^{-2}	Weight of deposit	5–6.0 mg cm^{-2}
Thickness of deposit	6.0–7.0 μm	Thickness of deposit	11–12 μm	Thickness of deposit	5–7 μm
Colour of deposit	Pale grey	Colour of deposit	Black	Colour of deposit	Bright white
Adhesion	Good	Adhesion	Very good	Adhesion	Very good

EPMA technique. The electron beam was fixed corresponding to the wavelength of the metals at a selected point on the surface and also scanned over a wide area to record the degree of homogeneity from the EPMA spectrum.

The XRD (X-ray diffraction) studies were carried out with cobalt-K_α radiation (A = 25 mA, KV = 35), in the range of 10^3 Hz, at a scan rate of 2° min^{-1}. The data derived from the diffraction patterns were compared with ASTM data to identify the phases present in Ni–Mo and Ni–W alloy coatings, and are presented in Table 2.

The chemical compositions of the alloy codeposits were estimated with the help of a Perkin–Elmer Atomic Absorption Spectrophotometer Model 380 (AAS) by chemical stripping of the deposits with acid solutions.

2.3. *Current–potential relationships*

The deposited electrodes were tested for the evaluation of electrochemical parameters, by exposing a geometric area of 8.0 cm^2. The experiments were carried out in a three-compartment stainless steel cell under galvanostatic steady state conditions. Two nickel plates with sufficiently large area, contained in Nylon bags, were used as auxiliary electrodes. As reference, a Hg/HgO, OH^- electrode in the working solution, linked to the main compartment via a Luggin capillary, was used. The potentiodynamic experiments were carried out using a PAR Model 370 Electrochemistry System. Alkaline solution (6 M) was prepared from analytical grade KOH pellets in triple distilled water and was pre-electrolysed for more than 48 h at 100 mA cm^{-2} between two platinum electrodes in order to eliminate the electroactive impurities. The working electrodes were precathodized at 1 mA cm^{-2} for 30 min at room temperature. The open circuit potentials were measured after 60 min at equilibrium conditions. The galvanostatic steady state potential values measured as a function of applied current densities were compensated for the IR components and used to construct the Tafel plots. The IR components were measured using an interruptor method.

2.4. *Reverse potential cycling (RPC) tests*

An accelerated experiment [10] was adapted to assess the stability of the present alloy coatings. The precathodized electrode was scanned potentiostatically to 200 mV, positive with respect to the reversible hydrogen electrode potential (RHEP) at 0.5 mV s^{-1}. The scan was then reversed at the same rate to 100 mV,

Table 2. XRD data obtained on Ni–Mo and Ni–W electrodeposits

Alloy/electrodeposit	*Measured d (nm)*	*Standard value d (nm) ASTM*	I/I_0	*hkl*	*Phase*
Nickel–molybdenum	0.203	0.205	100	211	
on mild steel	0.134	0.133	40	222	$MoNi_4$
	0.117	0.116	50	103	(Tetragonal)
	0.265	0.272	40	111	
	0.143	0.140	5	220	MoO_3 (Orthorhombic)
Nickel–tungsten on	0.203	0.203	100	211	Ni
mild steel	0.156	0.158	76	210	W
	0.174	0.172	65	111	WO_2

negative with respect to RHEP. This cycling process was continued until a significant change in the behaviour was observed. A plot of the limiting oxidation current densities as a function of the number of cycles was constructed.

2.5. *Time varition analysis*

Here, the experiments were carried out in a three-compartment 10 litre capacity stainless steel tank containing 8 litres of the same alkaline solution. The time variation effect of the cathode potential was studied by applying a constant cathodic current density for a long time with periodic replenishment of the electrolyte with triple distilled water to the original volume to balance the water lost on electrolysis. The accelerated life tests were carried out by suddenly raising the current density value to a specific value at regular time intervals of 5 days and monitoring the shift in the potential with time for 5 h. The simulation experiments were performed by subjecting the cathodes to common industrial conditions. The circuit was interrupted over time intervals ranging from 5 to 10 days and again closed to test the effect of such severe but common incidents on the cathode potential in industrial water electrolysis.

2.6. *Thermal activation procedures*

As inclusion codeposits are likely in any alloy electrodeposition involving transition metals, such as molybdenum and tungsten [11], the thermal activation of such systems at high temperatures in a hydrogen atmosphere was found [12] to improve their catalytic properties. Hence the deposited samples were laid down in an alumina tube, placed inside a glove box made of stainless steel and subjected to thermal activation in a hydrogen atmosphere in the temperature range 573 to 1073 K for various times. The effect of this treatment on the catalytic properties was investigated by applying a constant cathodic current of density 300 mA cm^{-2} at typical electrolyser operation conditions for 6 h and measuring the cathode potential at the end of this period. The data presented in Table 3 were obtained by testing three identical test pieces in each category and the values were not compensated for IR components.

*Table 3. Effects of thermal activation in H_2 atmosphere on the catalytic activities of alloy coatings**

Alloy/codeposit	*Temperature (K)*	*Duration (h)*	*$-E$ (300) at 353 K (mV)*	*$-\eta$ (300) at 353 K (mV)*
Ni–Mo	573	5	1134	204
	773	5	1125	195
	1073	5	1080	150
	1073	10	1077	147
Ni–Zn (after leaching	1073	5	1140	210
Zn in KOH)	1073	10	1130	200
Ni–Co	1073	5	1180	250
	1073	10	1178	248
Ni–W	1073	5	1200	270
	1073	10	1185	255
Ni–Fe	1073	5	1225	300
	1073	10	1217	292
Ni–Cr	1073	5	1355	420
Ni plated mild steel	1073	5	1420	490

* E and η values are not compensated for IR, and were obtained at 300 mA cm^{-2}.

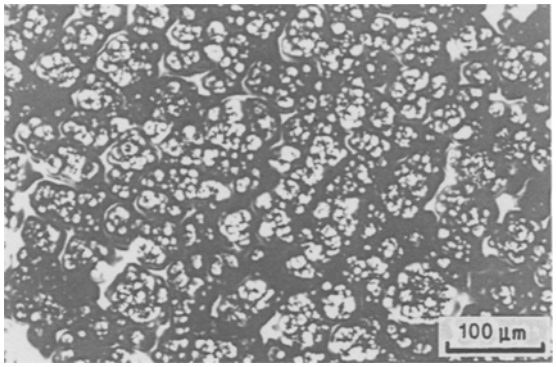

Fig. 1. Scanning electron micrograph of Ni–Mo alloy surfaces as deposited.

3. Results and discussion

3.1. *Physical characteristics of the coatings*

The feasibility of codeposition of metals like Mo, W, Co, Fe, Zn and Cr along with Ni is well established [13–17] although Mo cannot be electrodeposited from aqueous solutions [18] as such. The thickness of the coatings ranged from 2.5 to 12 μm for the present group of binary deposits.

The scanning electron micrographs of the surfaces of Ni–Mo alloy electrodeposits as deposited and after continuous cathodic polarization for about 1500 h are shown in Figs 1 and 2. The appearance of minor cracks after prolonged use may be due to the time-dependent influence of the entrapped tiny bubbles of the evolved hydrogen. The microstructures of the deposits undergo significant changes with time while under operation. Further, the influence of the impurities that arise from the cell components [19] and which are deposited at the cathode surface has led to electrocatalytic inhibition of the active alloy component and thus resulted in slow variation in the potential values with time. Figure 3 shows the time variation effects of the cathode potentials for the alloy deposits on continuous operation.

3.2. *Chemical composition and crystal structure of the coatings*

The EPMA spectra exhibited a regular distribution pattern of the alloying metals on the alloy surfaces of Ni–Mo, Ni–Fe, Ni–Co and Ni–W. The chemical compositions of the alloy coatings were found to be 75 % Ni, 20 % Mo for Ni–Mo; 80 % Ni, 18 % Fe for Ni–Fe; 54 % Ni, 45 % Co for Ni–Co; 73 % Ni, 25 % W for Ni–W; 60 % Ni, 40 % Zn for Ni–Zn; and 90 % Ni, 7 % Cr for Ni–Cr by gram atomic weight. The XRD pattern obtained for Ni–Mo and Ni–W were analysed; the crystal structure of the active phase for Ni–Mo was identified to be $MoNi_4$ with tetragonal geometry. The crystal structure of the inclusion codeposit, MoO_3 was found to be orthorhombic.

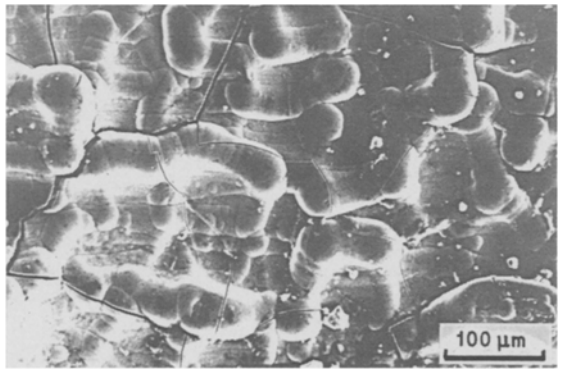

Fig. 2. Scanning electron micrograph of Ni–Mo alloy cathode surface after 1500 h of electrolysis.

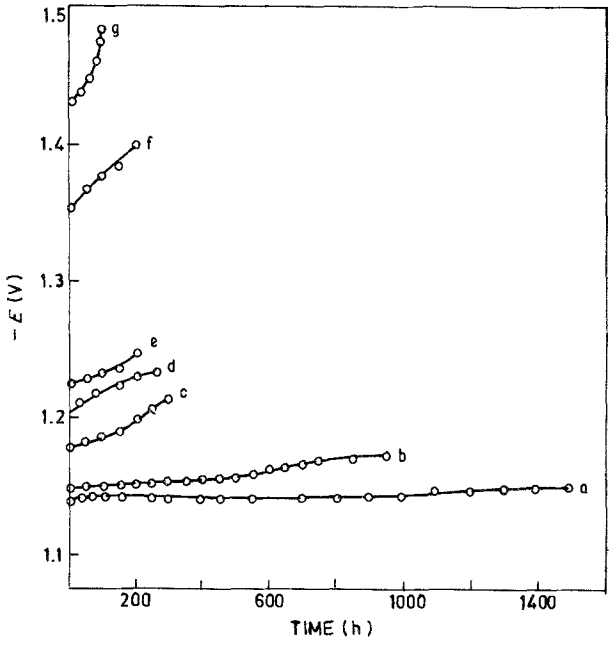

Fig. 3. Time variation effects of the cathode potentials at 300 mA cm^{-2} and at 353 K in 6 M KOH (a) Ni–Mo; (b) Ni–Zn (after leaching Zn); (c) Ni–Co; (d) Ni–W; (e) Ni–Fe; (f) Ni–Cr; (g) Ni-plated mild steel.

3.3. *Reverse potential cycling (RPC) tests*

The behaviour of Ni–Mo and Ni–W with respect to the hydrogen oxidation potentials were the same, but the corresponding currents differed slightly. In general, the alloy coatings did not undergo oxidation up to 200 mV positive to the RHEP, which was evident from the flat portion of the curve shown in Fig. 4. The behaviour of Ni–Mo deposit, when compared with that of the other binary deposits considered in this work, indicates stronger hydrogen adsorption on Ni–Mo deposit leading to higher hydrogen oxidation currents. As the magnitude of these currents is not high enough [9] to represent the oxidation of the electrode and does not vary much on repeated cycling, it is obvious that these currents represent the oxidation of the dissolved and adsorbed hydrogen on the electrode surface. Since it is unlikely that a cathode in a unipolar water electrolyser would ever experience a potential as high as this, this test is sufficient to evaluate their stability under open circuit conditions. The results reported in this work do not agree with the results of other similar work [9], possibly owing to the

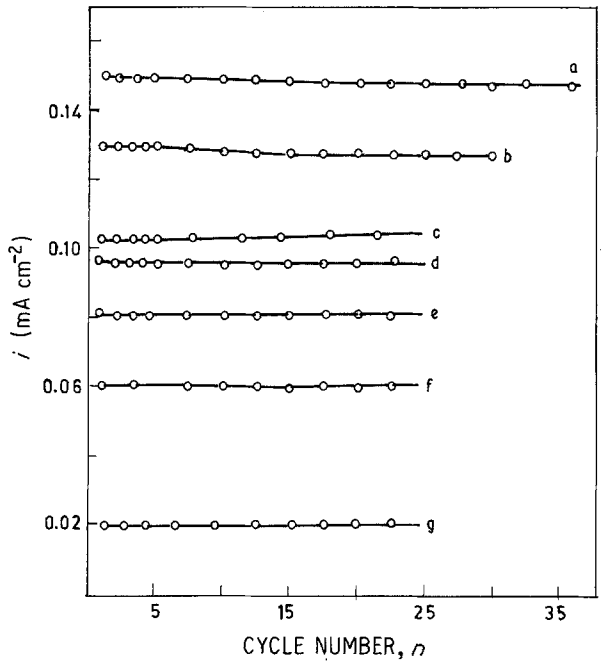

Fig. 4. Plot of anodic limiting oxidation currents observed in the reverse potential cycling experiments against the number of cycles in 6 M KOH at 301 K and at −0.85 V against Hg/HgO, OH^-; (a) Ni-Mo; (b) Ni-W; (c) Ni-Co; (d) Ni-Fe; (e) Ni-Cr; (f) Ni-Zn; (g) Ni-plated mild steel.

very short delay of the cathode at +200 mV to the open circuit potential.

3.4. *Life tests by simulation experiments*

The results of accelerated life tests carried out on the Ni-Mo cathode indicated that the variation in the cathode potential is 30 mV over a period of 60 days at 600 mA cm^{-2} and at 353 K. The results obtained on Ni-Co, Ni-W, Ni-Fe and Ni-Zn (after leaching Zn in KOH) indicate a variation of about 60 mV over a period of about 10 days. This means that the electrochemical behaviour of the deposits was modified significantly under these accelerated test conditions involving vigorous gas evolution, which may arise accidentally in commercial cells. The simulation experiments indicated a jump of 60 mV in the open circuit potential value over an interruption duration of 15 days on Ni-Mo cathodes, which means that the adsorbed hydrogen gets desorbed from the surface slowly with time. The results of simulation experiments on other deposits under identical conditions indicated wide variation (e.g., 150 mV on Ni-W; 110 mV on Ni-Co) in the cathode potential. The interesting point here is that the original potential values were again established by subjecting the cathodes to a current density of 0.1 μA cm^{-2} for some time (60 min). From this, it is concluded that the open circuit stability can be conserved by applying a negligibly small cathodic current density while they are not in use [2].

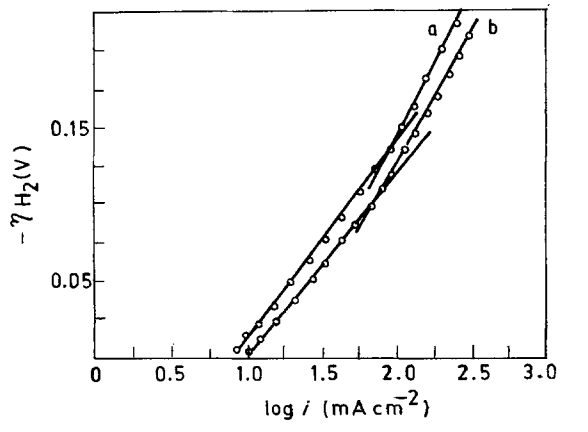

Fig. 5. Tafel plots of the h.e.r. on Ni-Mo alloy electrodeposits (a) at 303 K, and (b) at 353 K in 6 M KOH.

3.5. *The hydrogen evolution reaction (h.e.r.) parameters*

Figure 5 shows the Tafel lines for a Ni-Mo alloy cathode. The Tafel lines for other alloys were also obtained (figures not shown) to derive the hydrogen evolution reaction parameters shown in Table 4. The following points can be made from these data:

1. All the binary alloy deposits, based on the transition metals considered here, exhibited electrocatalytic activity towards the h.e.r.

2. The cathodic contribution to the electrolyser voltage can be reduced by 0.3 V under typical industrial conditions by employing the Ni-Mo cathode in the place of conventional mild steel cathodes.

3. The Tafel slope values for the deposits Ni-Co, Ni-W, Ni-Zn and Ni-Fe under low polarization conditions ($i < 50$ mA cm^{-2}) ranges from 30 to 50 mV dec^{-1}; the values for Ni-Mo and Ni-Cr under these conditions range from 110 to 150 mV dec^{-1}. Under high polarization conditions, the values range from 135 to 190 mV dec^{-1} for Ni-Mo, Ni-Zn Ni-Fe and Ni-Cr; the values for Ni-Co and Ni-W under these conditions were above 200 mV dec^{-1}.

4. The apparent energy of activation for the h.e.r.

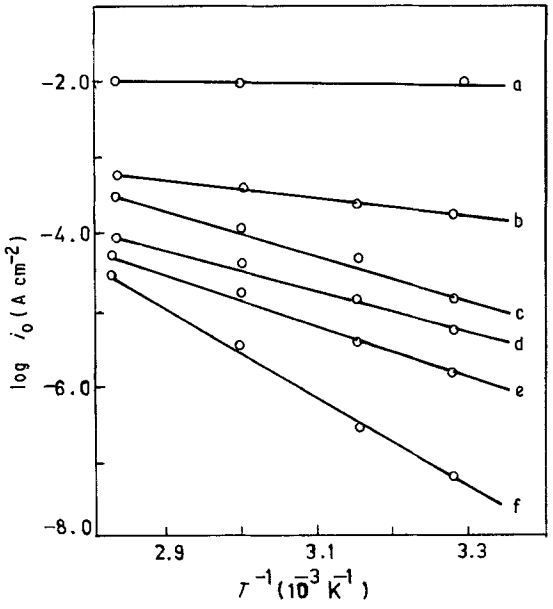

Fig. 6. Arrhenius plots of the h.e.r. on alloy deposits, under low polarization conditions: (a) Ni-Mo; (b) Ni-Cr; (c) Ni-W; (d) Ni-Zn (after leaching Zn); Ni-Fe; (f) Ni-Co.

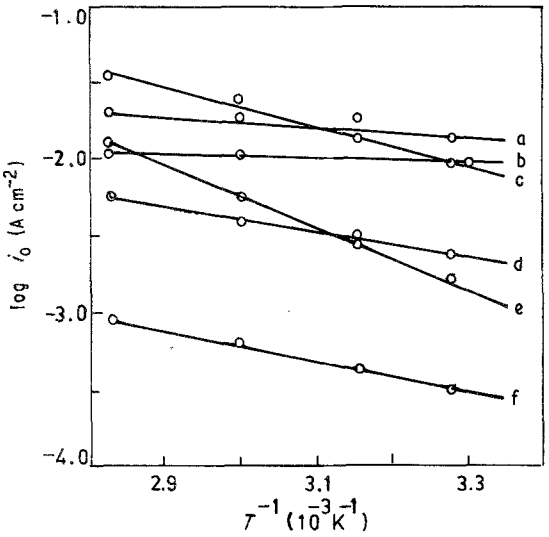

Fig. 7. Arrhenius plots of the h.e.r. on alloy deposits under high polarization conditions: (a) Ni–W; (b) Ni–Mo; (c) Ni–Co; (d) Ni–Fe; (e) Ni–Zn; (f) Ni–Cr.

on the alloy deposits obtained from the Arrhenius plots (see Figs 6, 7 and Table 4) are very low in magnitude compared with that for pure nickel and many other systems [15, 20].

The magnitude of the Tafel parameters (30 to 50 mV dec^{-1}) obtained for the deposits Ni–Co, Ni–W, Ni–Zn and Ni–Fe under low polarization conditions ($i < 50\,\text{mA cm}^{-2}$) agree well with the values of other authors obtained on transition metal-based coatings, that is on Ni–Fe eletrodeposits [20] and Ni–Mo thermal deposits [21]. The corresponding values obtained on Ni–Mo and Ni–Cr electrodeposits in the present work (110 to 150 mV dec^{-1}) are not in agreement with the results of similar electrodes, for example, Ni–Mo–Cd coatings [22, 23]. The very low values reported by these authors (30 to 38 mV dec^{-1}) were estimated in the current density region from 0.01 mA cm^{-2} to 30 mA cm^{-2}. However, in view of the common practical alkaline water electrolysis conditions, namely, $300\,\text{mA cm}^{-2} > i > 10\,\text{mA cm}^{-2}$, in the present work the Tafel parameters reported were obtained under these conditions. The values obtained under high polarization conditions ($i > 100\,\text{mA cm}^{-2}$) vary significantly among the various binary deposits. The ΔE values suggest that the present results reflect changes in the surface coverage of the adsorbed hydrogen as a function of which of the binary components are chosen with nickel. Thus, no correlation exists among the d-band structures of the constituent metals and the ΔE values.

3.6. *Catalytic activation effects*

As transition metals such as Ni, Fe, Co and W are prone to oxidation, the effect of thermal pretreatment of various binary coatings in a hydrogen atmosphere on the catalytic activities for the cathodic hydrogen

Table 4. Electrochemical parameters for the h.e.r. on different cathode materials

Substrate	*Alloy coating*	*Temp. (K)*	*b(mV dec^{-1})*		*ΔE (kJ mol^{-1})*		*$-\eta H_2$ (mV) at 300 mA cm^{-2}*
			$i < 50\,\text{mA cm}^{-2}$	*$i > 100\,\text{mA cm}^{-2}$*	*$i < 50\,\text{mA cm}^{-2}$*	*$i > 50\,\text{mA cm}^{-2}$*	
Mild steel	Ni–Mo	303	110	170	2.3	2.0	200
		333	112	172			192
		353	112	175			185
Mild steel	Ni–Zn (after leaching Zn in KOH)	305	30	135	52.63	38.28	425
		318	35	155			360
		333	50	170			265
		353	50	175			225
Mild steel	Ni–Co	305	30	285	109.33	24.22	380
		318	30	270			350
		333	30	255			300
		353	35	245			240
Mild steel	Ni–W	305	25	315	58.03	7.66	470
		318	35	335			410
		333	35	235			285
		353	25	225			280
Mild steel	Ni–Fe	305	50	190	63.8	17.06	410
		318	35	175			360
		333	30	155			310
		353	25	150			270
Mild steel	Ni–Cr	305	160	190	22.17	19.49	550
		318	150	180			500
		333	150	175			460
		353	150	170			445
Mild steel		305	125	110	59.8	68.1	620
		318	130	112			575
		333	130	115			550
		353	135	125			540

evolution from alkaline solutions was investigated. The results are presented in Table 3 and the following points are obvious:

(a) In general, the hydrogen overpotential values are lower in the case of activated surfaces when compared with unactivated surfaces.

(b) A reduction of 50 mV in the hydrogen overpotential is possible under the optimun treatment conditons, namely, thermal activation at 1073 K for 5 h in a hydrogen atmosphere on a Ni–Mo cathode.

(c) The treatment at still higher temperatures, or for a long time at the optimum temperature, does not help much (results not shown in Table 3).

4. Conclusions

From the present results, we conclude that Ni–Mo alloy coatings, obtained from an alkaline citrate bath, on mild steel substrates offer a cost effective and promising cathode for energy efficient alkaline water elecltrolysis. The hydrogen adsorption characteristics of the present alloy deposits differ significantly from those of the constituent metals, an experimental observation which opens up a wide range of detailed research to identify the best electrocatalytic surface for the economical production of hydrogen.

References

[1] I. Arul Raj and V. K. Venkatesan, *Int. J. Hydrogen Energy* **13** (1988) 215.
[2] *Idem, Trans. SAEST* **22** (1987) 189.
[3] I. Arul Raj, K. Venkateswara Rao and V. V. Venkatesan, *Bull. Electrochem.* **2** (1986) 157.
[4] D. E. Hall, J. M. Sarver and D. O. Gothard, *Int. J. Hydrogen Energy* **13** (1988) 547.
[5] J. Divesk, P. Malinowski, J. Margel and H. Schmitz, *ibid.* **13** (1988) 141.
[6] M. R. Gennero de Chialvo and A. C. Chialvo, *Electrochim. Acta* **33** (1988) 825.
[7] G. Fiori and C. M. Mari, *Int. J. Hydrogen Energy* **12** (1987) 159.
[8] M. M. Jaksić, *ibid.* **12** (1987) 727.
[9] D. E. Brown, M. N. Mahmood, M. C. M. Man and A. K. Turner, *Electrochim. Acta* **29** (1984) 1551.
[10] M. B. Janjua and R. L. Le Roy, *Int. J. Hydrogen Energy* **10** (1985) 11.
[11] A. Brenner, in 'Electrodeposition of Alloys, Principles and Practice', Vol. 2, Academic, New York (1963) p. 430.
[12] H. Wendt and V. Plzak, *Electrochim. Acta* **28** (1983) 27.
[13] E. Beltowska-Lehman and K. Vu Quang, *Surf. Coat. Technol.* **27** (1986) 75.
[14] C. Karwas and T. Hepel, *J. Electrochem. Soc.* **135** (1988) 839.
[15] D. E. Hall, *ibid.* **128** (1981) 740.
[16] P. W. T. Lu and S. Srinivasan, *ibid.* **125** (1978) 265.
[17] B. Tereszko, A. Risenkampf and K. Vu Quang, *Surf. Coat. Technol.* **12** (1981) 301.
[18] A. T. Wasko, 'Electrochimia molibdena i wolframa', Izd. Naukowa Dunka, Kiev (1977).
[19] A. Nidola and R. Schira, in Proceedings of the Symposium Advances in Chlor Alkali and Chlorate Industry (edited by E. M. Spore and M. M. Silver), The Electrochemical Society, Pennington, New York (1984) p. 206.
[20] E. R. Gonzales, L. A. Avaca, A. Carubelli, A. A. Tanaka and G. Tremiliosi – Filho, *Int. J. Hydrogen Energy* **9** (1984) 689.
[21] D. E. Brown, M. N. Mahmood, A. K. Turner, S. M. Hall and P. O. Fogarty, *ibid.* **7** (1982) 405.
[22] B. E. Conway, H. Angerstein-Kozlowska, M. A. Sattar and B. V. Tilak, *J. Electrochem. Soc.* **130** (1983) 1825.
[23] B. E. Conway and L. Bai, *Int. J. Hydrogen Energy* **11** (1986) 533.